Published in final edited form as:
Biochim Biophys Acta. 2010 February ; 1798(2): 216–222. doi:10.1016/j.bbamem.2009.08.020.

Partitioning, dynamics, and orientation of lung surfactant peptide KL_4 in phospholipid bilayers

Joanna R. Long, **Frank D. Mills**, **Omjoy K. Ganesh**, **Vijay C. Antharam**, and **R. Suzanne Farver**
Department of Biochemistry and Molecular Biology and McKnight Brain Institute, Box 100245, Gainesville, FL 32610-0245

Summary

Lung surfactant protein B (SP-B) is a lipophilic protein critical to lung function at ambient pressure. KL_4 is a 21-residue peptide which has successfully replaced SP-B in clinical trials of synthetic lung surfactants. CD and FTIR measurements indicate KL_4 is helical in a lipid bilayer environment, but its exact secondary structure and orientation within the bilayer remain controversial. To investigate the partitioning and dynamics of KL_4 in phospholipid bilayers, we introduced CD_3-enriched leucines at four positions along the peptide to serve as probes of sidechain dynamics via ^2H solid-state NMR. The chosen labels allow distinction between models of helical secondary structure as well as between a transmembrane orientation or partitioning in the plane of the lipid leaflets. Leucine sidechains are also sensitive to helix packing interactions in peptides that oligomerize. The partitioning and orientation of KL_4 in DPPC/POPG and POPC/POPG phospholipid bilayers, as inferred from the leucine sidechain dynamics, is consistent with monomeric KL_4 lying in the plane of the bilayers and adopting an unusual helical structure which confers amphipathicity and allows partitioning into the lipid hydrophobic interior. At physiologic temperatures, the partitioning depth and dynamics of the peptide are dependent on the degree of saturation present in the lipids. The deeper partitioning of KL_4 relative to antimicrobial amphipathic α-helices leads to negative membrane curvature strain as evidenced by the formation of hexagonal phase structures in a POPE/POPG phospholipid mixture on addition of KL_4. The unusual secondary structure of KL_4 and its ability to differentially partition into lipid lamellae containing varying levels of saturation suggest a mechanism for its role in restoring lung compliance.

Keywords

KL_4; sinapultide; lucinactant; lung surfactant; surfactant protein B; respiratory distress syndrome; lipid bilayers; ^2H NMR; leucine sidechain dynamics

Introduction

Lung surfactant is a highly organized, lipid rich fluid which lines the highly curved alveoli and lowers surface tension. Lung surfactant protein B (SP-B) is an extremely hydrophobic protein which is critical to the proper trafficking of lipids in lung surfactant and establishment of a stable air-water interface [1,2]. Mature SP-B is a homodimer with two 79–81 amino acid

Address correspondence to: Dr. Joanna R. Long, Box 100245, Department of Biochemistry and Molecular Biology, University of Florida, Gainesville, FL 32610-0245 Telephone: 352-846-1506, Fax: 352-392-3422. Corresponding author's: jrlong@mbi.ufl.edu.

disulfide-linked subunits containing high levels of valine, leucine, isoleucine, proline, alanine, phenylalanine, and tryptophan [3–5]. Each monomer contains an additional six cysteines that form intramolecular disulfide bonds and their pattern of disulfide formation along with lipophilicity place SP-B in the saposin family of proteins. The hydrophobicity and disulfide bridges in SP-B also make purification or heterologous expression of the protein in large quantities impractical. Synthetic, peptide-based lung surfactant replacements for treatment of RDS have shown promise and would remove the immunologic risks associated with current therapies utilizing animal-derived lung surfactant [6–8].

Much of the activity of SP-B in altering lipid organization and dynamics can be recapitulated by the N- and C-terminal 20–25 amino acid fragments of SP-B [4,9]. Both peptides form helices in lipid environments[10–13], but their individual roles in lipid trafficking are not well understood. While both peptides have considerable surface activity, activity similar to native SP-B has only been achieved with a chimeric construct of the two peptides [14]. The C-terminus contains many leucines and lacks aromatic residues while the N-terminus contains four prolines as well as a phenylalanine and a tryptophan. The peptides also have different spacings of hydrophilic and hydrophobic amino acids. These differences could lead to subtle variations in secondary structure and partitioning into lipid lamellae as well as different effects on phospholipid dynamics.

The C-terminus of SP-B served as the template for designing the KL_4 peptide, KLLLLKLLLLKLLLLKLLLLK [8], which to date has shown the greatest clinical success for treatment of respiratory distress syndrome (RDS) with synthetic surfactant [15–19]. The basis for the primary sequence of KL_4 was the charge distribution and hydrophilic/hydrophobic ratio within $SP\text{-}B_{59–80}$. However, their primary sequences have only modest similarity. KL_4 has also been found via CD and FTIR to adopt a helical conformation in a lipid environment [20–22], but the periodicity of the charged lysine residues is at odds with the peptide adopting a canonical α-helical conformation (3.6 residues/turn) which is either amphipathic, for partitioning at the lipid interface, or which can span the lipid bilayer in a TM orientation without burying lysine sidechains in the hydrophobic interior of the bilayer. An early FTIR study of KL_4 in DPPC/DPPG concluded the peptide formed a helix spanning the bilayers and posited that KL_4 might more closely mimic lung surfactant protein C (SP-C) rather than the C-terminus of SP-B [20]. More recent IR studies of KL_4 conclude that it binds to the lipid interface but its structure and penetration are lipid and pressure dependent [23]. An assay of the ability of KL_4 to cross ER microsomal membranes via translocon-mediated translation in an in vitro transcription-translation system demonstrated that when KL_4 is expressed within a membrane protein host it can span phospholipid bilayers [24]. While all of these experiments are well-suited for analyzing peptides which clearly form amphipathic or TM α-helics, they are inherently low resolution and are also sensitive to sample conditions (hydration and P/L ratio in the case of FTIR and flanking protein sequences and integrity of the microsomal membranes in the case of the in vitro translation assay). Additionally, many of the published studies have been carried out at room temperature, well below the melting temperature of DPPC (the primary lipid in lung surfactant) or even lung surfactant itself, and with P/L ratios that are much higher than is clinically relevant, raising the possibility of peptide aggregation.

We have been utilizing solid-state NMR spectroscopy to gain a higher resolution understanding of the structure of KL_4 and its effects on lipid organization under physiologically relevant conditions. In particular, the structure of KL_4 in 4:1 DPPC/POPG and 3:1 POPC/POPG lipid mixtures and its effects on phospholipid dynamics have been characterized. The former lipid composition is similar to formulations commonly used in synthetic lung surfactant, while the latter is a paradigm lipid system commonly employed to probe peptide/lipid interactions, particularly in studies of cationic, amphipathic helices [25–27]. Lipid phases of either of these

compositions could also be found in localized areas of the alveoli during the breathing cycle [28].

With ^{2}H and ^{31}P solid-state NMR we have established that the lipids remain in lamellar phases up to 5 mol% KL_4 with no evidence of phase separation at physiologic (37 °C) temperature. The effects of KL_4 on the two lipids systems vary with the fatty acyl chains in the DPPC/POPG mixture becoming more ordered on addition of peptide while the hydryophobic interior of the POPC/POPG bilayers becomes more disordered. Based on order parameter analyses, we interpreted these observations as the peptide partitioning more deeply into the DPPC/POPG bilayers [29].

High-resolution measurements on KL_4 in POPC/POPG bilayers via magic angle spinning dipolar recoupling experiments indicate the peptide adopts an amphipathic helical structure due to the backbone torsion angles diverging from canonical values (e.g. −65, −45) in the lipid environment to form a helix with a lower angle of rotation per residue and (ϕ, ψ) torsion angles that average (−105°, −30°) [22]. More recent measurements on KL_4 in DPPC/POPG suggest the peptide can form a helix which has an even lower angle of rotation, increasing its amphipathicity and allowing it to more deeply partition into the lipid interior without adopting a TM orientation (Figure 1c; A.K. Mehta and J.R. Long, submitted). However, these measurements rely on determining the relative orientations of $^{13}C'$ chemical shift anisotropy tensors, which have degeneracies in particular regions of (ϕ, ψ) space, making it difficult to distinguish between a canonical α-helix (−63°, −45°) and a more amphipathic helix (−63°, −81°). Molecular dynamics simulations, coupled with ssNMR measurements of inter-residue $^{13}C' \rightarrow ^{15}N$ distances and CD spectra, indicate the (−63°, −81°) conformation is correct, but more conclusive data is needed. Additionally, the orientation of the KL_4 helix relative to the bilayer normal in DPPC/POPG lipids cannot be conclusively determined from the lipid dynamics measurements. Moreover, structural characterization via dipolar recoupling experiments requires the removal of dynamics, via flash-freezing and lyophilization, removing any information on the dynamics of the peptide which might be important to its function.

Based on the helical models for KL_4 in DPPC/POPG and POPC/POPG (Figure 1), we chose to examine the sidechain dynamics of four leucines in KL_4 as a function of temperature and lipid composition. The four positions were selected to be sensitive to both helix pitch and the orientation of KL_4 within the lipid bilayers as well as to provide insight into how the dynamics of the peptide might play a role in its function. Leucine residue dynamics are also sensitive to peptide oligomerization [30], allowing us to determine whether KL_4 is monomeric under physiologically relevant conditions. This is particularly of interest given the propensity of leucine residues to enhance peptide oligomerization in membranes [31,32]. Variations in temperature allow us to monitor the partitioning of KL_4 in both fluid and gel phase lipid bilayers to infer how its structure, orientation, and organization might vary between the different sample conditions used in previous studies.

A particular advantage of probing peptide dynamics via ^{2}H NMR is it enables us to study KL_4 under close to physiologic conditions, with full hydration of the lipids, and over a range of temperatures relevant to the phase properties of the lipids. This allows us to assay whether structural measurements, carried out on samples in which dynamics are removed by flash freezing samples and subsequent lyophilization, are consistent with the structure and dynamics of the peptide under more physiologically relevant conditions. It also allows us to monitor the interplay between peptide partitioning, lipid dynamics, peptide secondary structure and dynamics, lipid polymorphisms, and temperature, providing important insights into lung surfactant function and more generally the enthalpic and entropic contributions underlying amiphathic peptides interactions with and influence on phospholipid assemblies.

Materials and Methods

Synthesis of KL_4

Selectively deuterated 5-d_3-L-leucine was purchased (Cambridge Isotopes, Andover, MA) and fmoc-protected using standard protocols [33]. Four variants of KL_4, each containing a single enriched leucine (at Leu3, Leu10, Leu12, or Leu19), were synthesized via solid-phase peptide synthesis on a Wang resin (ABI 430, ICBR, UF), cleaved from the resin with 90% TFA/5% triisopropyl-silane/5% water and ether precipitated. The cleaved product was purified via RP-HPLC using a C18 Vydac column with a water/acetonitrile gradient (containing 0.3% TFA). The fractions corresponding to KL_4 were collected and purity of the product was verified by mass spectrometry with a single species of MW=2572. Dried peptide was weighed and dissolved in methanol to a stock concentration of approximately 1 mM, and aliquots were analyzed by amino acid analysis for a more accurate determination of concentration and to verify purity (Molecular Structure Facility, UC Davis)

Preparation of Peptide:Lipid Samples

POPC, DPPC, and POPG were purchased as chloroform solutions (Avanti Polar Lipids, Alabaster, AL) and concentrations were verified by phosphate analysis [34] (Bioassay Systems, Hayward, CA). The lipids were mixed at a molar ratio of 4:1 DPPC/POPG and 3:1 POPC/POPG in chloroform and aliquoted. For samples containing peptide, a methanol solution of KL_4 was added to lipid solutions with final protein/lipid (P/L) molar ratio of 1:50 to match the clinical formulation of KL_4. The samples were dried under a stream of nitrogen with the sample temperature maintained at 42–50° in a water bath; the resulting films were suspended in warm cyclohexane, flash-frozen, and lyophilized overnight to remove residual solvent.

Solid state NMR analysis

For each solid-state NMR sample, 20–30 mg of peptide-lipid powder was placed in a 5 mm diameter NMR tube and 200 μL of buffer containing 5 mM HEPES at pH 7.4, 140mM NaCl, and 1mM EDTA in ^2H depleted water (Cambridge Isotopes, Andover, MA) was added. NMR samples were then subjected to 3–5 freeze-thaw cycles with gentle manual agitation to form MLVs. ^2H NMR data were collected on a 500 MHz Bruker Avance system (Billerica, MA) using a standard high resolution 5 mm broadband probe and a quad echo sequence (90°-τ-90°-τ-acq with $\tau = 30\mu s$) with a B_1 field of 40 kHz. Spectra were acquired with 100,000–400,000 transients, a 0.2 second recycle delay time, and 500 kHz sweep width. Prior to Fourier transformation, spectra were phased, symmetrized by adding the complex conjugate, and damped with 200 Hz line exponential line broadening (or 500 Hz for low signal spectra at the lowest temperature), with removal of signal between ±200 Hz (±500 Hz) ascribed to residual ^2H_2O. Spectra were acquired over a temperature range of −10 to 40 °C. Unsymmetrized spectra without solvent removal are available in Supporting Information. ^{31}P NMR data were collected on a 600 MHz Bruker Avance system (Billerica, MA) using a standard 5 mm BBO probe. Proton decoupling (25 kHz) was employed during acquisition to remove dipolar couplings. Spectra were acquired with 512–1024 scans and a 5 second recycle delay between scans to minimize RF sample heating. Chemical shift referencing is relative to an external phosphate buffer standard.

Results

Leucine sidechain dynamics for KL_4 in POPC/POPG lipid vesicles

^2H solid-state NMR spectra for Leu3, Leu10, Leu12, and Leu19 in 3:1 POPC/POPG as a function of temperature and label position are shown in Figures 2 and 3. First moment analyses of the spectra are provided in the supplementary information. The gel → liquid crystalline

phase transition temperature of this lipid mixture is −3 °C. At temperatures near the phase transition temperature, the Leu3 and Leu12 positions exhibit less dynamics relative to the Leu10 and Leu19 positions. The breadth and shape of the Leu3 and Leu12 powder patterns at −10 °C are consistent with the deuterated leucine methyl groups solely undergoing 3-fold rotation about the C_γ — C_δ bond; the Leu10 and Leu12 lineshapes are consistent with additional motion about the C_β — C_γ and/or C_α — C_β bonds [30, 35, 36]. At 0 °C the Leu3 and Leu12 positions begin to exhibit dynamics about the C_β — C_γ or C_α — C_β bonds but they are more limited relative to the Leu10 and Leu19 positions. In contrast, at 14 °C the lineshapes for Leu3, Leu12, and Leu19 have significantly narrowed relative to the Leu10 position. The dissimilarity in dynamics of the Leu10 and Leu 12 residues as well as the differences between Leu3 and Leu19 clearly rule out a TM orientation in the POPC/POPG lipid bilayers at all the monitored temperatures. Due to the phase transition temperature of the lipids being similar to the freezing point of water, with significant dynamics remaining only in the hydrophobic interior of the lipid bilayers at −10 °C, we interpret the contrast in dynamics between Leu3 and Leu10 relative to Leu12 and Leu19 as a function of temperature as the Leu3 and Leu10 positions partitioning closer to the lipid/water interface while the Leu12 and Leu19 positions partition more deeply into the hydrophobic interior of the lipid bilayers. The correlation of dynamics between the Leu10 and Leu19 positions as well as between the Leu12 and Leu3 positions are also more consistent with the helical model shown in Figure 1c rather than a canonicalα-helix (Figure 1a), which would predict correlations between Leu3 and Leu10 and between Leu12 and Leu19 if the helix axis lay in the plane of the lipid leaflet.

At higher temperatures (14 and 25 °C), the Leu3, Leu12 and Leu19 spectra exhibit line-shapes consistent with more motion about the C_β — C_γ and/or C_α — C_β bonds, while the Leu10 position still exhibits limited dynamics. This is consistent with the Leu10 position partitioning more deeply into the lipid interior while the Leu3, Leu12, and Leu19 residues partition at the lipid interface and is predicted by the helical structure observed for KL_4 at ambient temperatures in POPC/POPG vesicles (Figure 1b). At 40 °C a small decrease in dynamics is observed for the Leu19 position while the Leu3 and Leu12 positions continue to show more motion. This is consistent with the peptide partitioning slightly deeper into the lipid interior, an entropically driven process due to the hydrophobicity of KL_4, resulting in a small change in helix pitch and subsequent increase in hydrophobic moment, as in the model shown in Figure 1c.

Leucine sidechain dynamics for KL_4 in DPPC/POPG lipid vesicles

^{2}H solid-state NMR spectra for Leu3, Leu10, Leu12, and Leu19 in 4:1 DPPC/POPG as a function of temperature and label position are shown in Figure 4; first moment analyses are provided in the supplementary information. The gel→liquid crystalline phase transition of this lipid mixture is at 36 °C [29]. Below the phase transition temperature (e.g. 25 °C), all four positions exhibit decreased dynamics consistent with the methyl groups undergoing 3-fold rotation about the C_γ — C_δ bond and limited motion about the C_β — C_γ and/or C_α — C_β bonds. The dynamics of the Leu12 position are slightly less restricted than the Leu 19 position, for which the spectrum has a lower first moment than the Leu3 and Leu10 positions, consistent with differences in partitioning. The dynamics of all four positions are similar to those seen in 3:1 POPC/POPG lipids at lower temperatures, as would be expected given the differences in the phase transition temperatures of the lipids.

Above the phase transition (40 °C), the Leu3 and Leu12 sidechains are much more dynamic while the Leu10 and Leu19 positions continue to exhibit only limited dynamics. The dissimilarity in dynamics of the Leu10 and Leu 12 residues as well as the differences between Leu3 and Leu19 also clearly rule out a TM orientation in DPPC/POPG lipids. The change in the relative dynamics of the four positions with the phase of the phospholipids suggests changes

in the partitioning and/or secondary structure of KL_4 with temperature and underscores the need to study KL_4 at physiologically relevant temperatures, particularly in DPPC-rich mixtures given its high transition temperature. The reduced dynamics at the Leu10 and Leu19 positions suggest they are partitioned into the hydrophobic interior of the lipid bilayers. The correlation of dynamics between the Leu10 and Leu19 positions as well as the Leu12 and Leu3 positions are again more consistent with the helical models shown in Figure 1c rather than a canonicalα-helix (Figure 1a) or the helix modeled in Figure 1b. The dynamics at 40 °C for all four positions in DPPC/POPG are attenuated relative to in POPC/POPG, consistent with the peptide partitioning more deeply into the DPPC/POPG hydrophobic interior as was previously inferred by examining the dynamics of the fatty acyl chains [29].

Partitioning of KL_4 into POPE/POPG lipid vesicles induces negative curvature strain

^{31}P solid-state NMR spectra of 3:1 POPE/POPG MLVs with and without 3 mol% KL_4 are shown as a function of temperature in Figure 5. At lower temperatures, the spectra are indicative of lamellar lipid structures. The average headgroup orientations of the PE and PG lipids relative to the membrane normal are similar, leading to a single lamellar lineshape for the mixture. For the sample containing only phospholipids, the MLVs align significantly in the strong magnetic field leading to a very strong signal at the perpendicular edge of the lineshape and almost no signal at the parallel edge. Addition of KL_4 leads to less lipid alignment and a more typical lamellar lineshape. The alignment of phospholipid vesicles at the field strengths utilized and the disruption of this alignment by KL_4 have been previously documented [29]. At higher temperatures, the phospholipids undergo a transition to an isotropic phase, as evidenced by the appearance of a resonance near 0 ppm at 55 °C for the sample containing only phospholipids. This transition is complete by 61 °C and further changes in the lineshape are not observed. However, for the POPE/POPG sample containing KL_4, the transition from a lamellar phase does not occur until above 61 °C, and the appearance of two separate spectral features is observed at 67 °C. The peak near 0 ppm is consistent with an isotropic phase, while the feature observed at −4 ppm is suggestive of an inverted hexagonal phase. Heating further to 80 °C confirms the formation of hexagonal phase structures with a clear spectral lineshape that is reversed relative to the lamellar lineshape and half its width. A significant fraction of the phospholipids remain in the isotropic phase, which can be expected given high percentage of POPG in the sample and the relatively low concentration of KL_4 relative to the phospholipids. The induction of hexagonal phase structures in POPE/POPG mixtures by KL_4 demonstrates that the peptide induces negative membrane curvature strain.

Discussion

Models for KL_4 secondary structure and partitioning into lipid bilayers are presented in Figure 6 [37]. Four possibilities are shown: an α-helix lying in the plane of the bilayers; an α-helix spanning the bilayer; an alternative helical structure, based on our NMR measurements of KL_4 in DPPC/POPG, lying in the plane of the bilayers; and the alternative helical structure spanning the bilayer. The 21-residue length of the KL_4 peptide is sufficient for it to span the lipid bilayers in a TM orientation, but it would require the burying of 2–3 lysine sidechains into the hydrophobic interior. While lysines have a lower energetic barrier for partitioning into lipid bilayers than other basic residues, a TM orientation is only possible if the hydrophobic interaction of the leucine sidechains and the overall secondary structure overcome this barrier. Previous studies of peptides containing similar percentages of leucines and lysines indicate a stable TM orientation can only be achieved when the lysines are distributed closer to the N- and C-termini [38]. Nonetheless, a recent in vitro transcription-translation assay found KL_4 is able to cross the membrane [24]. However, this assay relies on the integration of KL_4 into the Escherichia coli inner membrane protein leader peptidase (Lep), which is translated in ER-derived microsomal membranes and the resulting protein is assayed for glycosylation after

proteinase K digestion. The assay is problematic in two regards. First, the flanking sequences of the Lep protein may influence the secondary structure of the integrated peptide. Second, KL_4 is known to influence lipid dynamics and trafficking and thus may affect the integrity of the microsomal membranes. Assuming an α-helical conformation, KL_4 possesses a low hydrophobic moment and the predicted ΔG_{app} for the KL_4 sequence inserting into ER membranes is −2.14 kcal/mol [24]. Conversely, if KL_4 assumes a structure with a lower helical pitch, its hydrophobic moment is increased by 3–4 kcal/mol and its insertion in a TM orientation is much less favorable (Figure 1b or 1c). Our structural studies of KL_4 interacting with POPC/POPG and DPPC/POPG vesicles suggest this latter scenario is correct for the peptide under fully hydrated conditions.

An alternative means to assay the orientation of KL_4 in lipid bilayers as well as its partitioning behavior is to examine the dynamics of the leucine sidechains at various positions in the peptide. The nonperturbing nature of incorporating ^2H into 5-d_3-L-Leucine and the increased sensitivity for ^2H solid-state NMR due to the three-fold rotation of the methyl group make this a particularly attractive probe for assaying dynamics. Previously, deuterated leucine has been utilized for examining dynamics and oligomerization of transmembrane sequences [30,35, 36]. However, to our knowledge, it has not been used to examine the partitioning of amphipathic helices into lipid bilayers. The frequency and symmetry of the leucines in the KL_4 sequence make the identification of a minimal number of sites for labeling particularly straightforward. To assay the orientation of the peptide, we chose two sites at the N- and C-termini (Leu3 and Leu19) as well as two sites which would be located near the center of the bilayer in a TM orientation (Leu10 and Leu12). Under all experimental conditions, the relative dynamics of these positions suggest a TM orientation is unlikely, particularly since the dynamics of Leu10 and Leu12 differ significantly. While packing of peptide helices in aggregates could lead to differences between these two positions, we do not see a loss of motion about the $C_\beta — C_\gamma$ and/or $C_\alpha — C_\beta$ bonds at any of the observed positions as would be expected for helix-helix packing interactions. Additionally, the dynamics observed at the various temperatures were easily reproduced regardless of the order in which spectra were collected consistent with all changes in dynamics being reversible and the samples being fully equilibrated.

Leucine sidechains are particularly sensitive to packing of side chains at helix interfaces. While we did not assay all possible helix interfaces in this study, the labels chosen lie at expected interfaces if the peptide were to oligomerize in the plane of the membrane. Above the gel → liquid crystalline phase transition temperature of the lipids, all samples exhibited leucine sidechain dynamics about the $C_\beta — C_\gamma$ and/or $C_\alpha — C_\beta$ bonds. This is in contrast to what has been observed for Leucines found at helix interfaces [30]. In our studies we have found KL_4 to form consistent secondary structure in phospholipids mixtures up to P/L ratios of 1:30. At 1:20, CD and FTIR spectra indicate the formation of β-sheet type structures consistent with aggregation of the peptide (K. Seu and S Decatur, personal communication).

As can be seen in Figure 1, differences in helix pitch lead to differences in the expected correlations between the labeled positions for the peptide lying in the plane of the lipid bilayer. For DPPC/POPG and POPC/POPG lipid mixtures near physiologic temperature, the correlation in sidechain dynamics among the four observed positions are consistent with a peptide having a high hydrophobic moment (Figure 1c), which agrees well with our structural measurements carried out on KL_4 in DPPC/POPG lipid vesicles (A.K. Mehta and J.R. Long, submitted). Near room temperature, the dynamics observed for KL_4 in POPC/POPG lipid vesicles correlate with the helical structure previously determined under the same conditions [22]. Based on these observations, only one of the four models in Figure 5 is consistent with out data near physiologic temperature, as indicated.

In this study, the dynamics observed for the KL_4 Leucine sidechains in DPPC/POPG containing samples are significantly attenuated relative to the POPC/POPG containing samples. This is consistent with previous observations that addition of peptide lowers the acyl chain order parameters in POPC/POPG lipid bilayers but increases the acyl chain order parameters in DPPC/POPG lipid bilayers [29]. This variation in partitioning depth is likely due to the unusual periodicity of the hydrophilic residues which confer temperature-dependent helical plasticity on partitioning of the peptide into lipid bilayers with varying levels of saturation.

Lipid polymorphisms that change the geometry and arrangement of lipid assemblies may be critical for lipid adsorption at the alveolar air-fluid interface [39]. The enrichment of DPPC at the air-water interface has been postulated as one of the major roles of SP-B. The KL_4 peptide's structural plasticity and variable penetration depth can affect the stability and composition of lung surfactant lipid structures by causing negative curvature strain as we have demonstrated in POPE/POPG phospholipid mixtures. These changes in curvature strain provide a mechanism for lipid trafficking from lamellar bodies and tubular myelin to the air-water interface in a manner that may select for DPPC.

Supplementary Material

Refer to Web version on PubMed Central for supplementary material.

Acknowledgments

The assistance of Dr. Alfred Chung in peptide synthesis and of the Molecular Structure Facility at University of California, Davis in AAA analysis is gratefully acknowledged. The research herein was funded by NIH 1R01HL076586 awarded to JRL. Support from the NSF National High Magnetic Field Laboratory and University of Florida is also gratefully acknowledged.

Abbreviations used

SP-B	surfactant protein B
RDS	respiratory distress syndrome
TM	transmembrane
NMR	nuclear magnetic resonance
CD	circular dichroism
FTIR	Fourier transform infrared spectroscopy
MLV	multilamellar vesicle
LUV	large unilamellar vesicle
L_α	fluid lamellar phase
L_β	gel lamellar phase
POPC	1-palmitoyl-2-oleoyl-*sn*-glycero-3-phospha-tidylcholine
POPE	1-palmitoyl-2-oleoyl-*sn*-glycero-3-phosphatidylethanolamine
POPG	1-palmitoyl-2-oleoyl-*sn*-glycero-3-phosphatidylglycerol
DPPC	1,2-dipalmitoyl-*sn*-Glycero-3-Phosphocholine
P/L	peptide/lipid molar ratio

References

1. Nogee LM, Demello DE, Dehner LP, Colten HR. Brief Report - Deficiency of pulmonary surfactant protein-B in congenital alveolar proteinosis. New Engl J Med 1993;328:406–410. [PubMed: 8421459]
2. Clark JC, Wert SE, Bachurski CJ, Stahlman MT, Stripp BR, Weaver TE, Whitsett JA. Targeted disruption of the surfactant protein B gene disrupts surfactant homeostasis, causing respiratory failure in newborn mice. Proc Natl Acad Sci 1995;92:7794–8. [PubMed: 7644495]
3. Sarin VK, Gupta S, Leung TK, Taylor VE, Ohning BL, Whitsett JA, Fox JL. Biophysical and biological activity of a synthetic 8.7-kDa hydrophobic pulmonary surfactant protein SP-B. P Natl Acad Sci 1990;87:2633–2637.
4. Revak SD, Merritt TA, Hallman M, Heldt G, Lapolla RJ, Hoey K, Houghten RA, Cochrane CG. The use of synthetic peptides in the formation of biophysically and biologically-active pulmonary surfactants. Ped Res 1991;29:460–465.
5. Johansson J, Curstedt T. Molecular structures and interactions of pulmonary surfactant components. Eur J Biochem 1997;244:675–93. [PubMed: 9108235]
6. Mingarro I, Lukovic D, Vilar M, Perez-Gil J. Synthetic pulmonary surfactant preparations: New developments and future trends. Curr Med Chem 2008;15:393–403. [PubMed: 18288994]
7. Seurynck SL, Patch JA, Barron AE. Simple, helical peptoid analogs of lung surfactant protein B. Chem Biol 2005;12:77–88. [PubMed: 15664517]
8. Cochrane CG, Revak SD. Pulmonary surfactant protein B (SP-B): structure-function relationships. Science 1991;254:566–8. [PubMed: 1948032]
9. Waring A, Taeusch HW. Interactions of surfactant peptides, SP-B and SP-C, with phospholipids using phospholipid spin labels. Clin Res 1989;37:A211–A211.
10. Bruni R, Taeusch HW, Waring AJ. Surfactant protein-B - lipid interactions of synthetic peptides representing the amino-terminal amphipathic domain. P Natl Acad Sci 1991;88:7451–7455.
11. Kang JH, Lee MK, Kim KL, Hahm KS. The relationships between biophysical activity and the secondary structure of synthetic peptides from the pulmonary surfactant protein SP-B. Biochem Mol Biol Int 1996;40:617–627. [PubMed: 8908373]
12. Booth V, Waring AJ, Walther FJ, Keough KMW. NMR structures of the C-terminal segment of surfactant protein B in detergent micelles and hexafluoro-2-propanol. Biochem 2004;43:15187–15194. [PubMed: 15568810]
13. Sarker M, Waring AJ, Walther FJ, Keough KMW, Booth V. Structure of mini-B, a functional fragment of surfactant protein B, in detergent micelles. Biochem 2007;46:11047–11056. [PubMed: 17845058]
14. Waring AJ, Walther FJ, Gordon LM, Hernandez-Juviel JM, Hong T, Sherman MA, Alonso C, Alig T, Braun A, Bacon D, Zasadzinski JA. The role of charged amphipathic helices in the structure and function of surfactant protein B. J Pep Res 2005;66:364–374.
15. Cochrane CG, Revak SD, Merritt A, Heldt GP, Hallman M, Cunningham MD, Easa D, Pramanik A, Edwards DK, Alberts MS. The efficacy and safety of KL_4-surfactant in infants with respiratory distress syndrome. Am J Resp Crit Care 1996;153:404–410.
16. Cochrane CG, Revak SD, Merritt TA, Schraufstatter IU, Hoch RC, Henderson C, Andersson S, Takamori H, Oades ZG. Bronchoalveolar lavage with KL_4-Surfactant in models of meconium aspiration syndrome. Ped Res 1998;44:705–715.
17. Wiswell TE, Smith RM, Katz LB, Mastroianni L, Wong DY, Willms D, Heard S, Wilson M, Hite RD, Anzueto A, Revak SD, Cochrane CG. Bronchopulmonary segmental lavage with surfaxin (KL_4-surfactant) for acute respiratory distress syndrome. Am J Resp Crit Care 1999;160:1188–1195.
18. Sinha SK, Lacaze-Masmonteil T, Soler AVI, Wiswell TE, Gadzinowski J, Hajdu J, Bernstein G, d'Agostino R, Dist STAR. A multicenter, randomized, controlled trial of lucinactant versus poractant alfa among very premature infants at high risk for respiratory distress syndrome. Pediatrics 2005;115:1030–1038. [PubMed: 15805381]
19. Ghodrat M. Lung surfactants. Am J Health Syst Pharm 2006;63:1504–21. [PubMed: 16896079]
20. Gustafsson M, Vandenbussche G, Curstedt T, Ruysschaert JM, Johansson J. The 21-residue surfactant peptide $(LysLeu_4)_4Lys$ (KL_4) is a transmembrane alpha-helix with a mixed nonpolar/polar surface. FEBS Lett 1996;384:185–8. [PubMed: 8612820]

21. Saenz A, Canadas O, Bagatolli LA, Johnson ME, Casals C. Physical properties and surface activity of surfactant-like membranes containing the cationic and hydrophobic peptide KL_4. FEBS J 2006;273:2515–27. [PubMed: 16704424]
22. Mills FD, Antharam VC, Ganesh OK, Elliott DW, McNeill SA, Long JR. The helical structure of surfactant peptide KL_4 when bound to POPC : POPG lipid vesicles. Biochem 2008;47:8292–8300. [PubMed: 18636713]
23. Cai P, Flach CR, Mendelsohn R. An infrared reflection-absorption spectroscopy study of the secondary structure in $(KL_4)_4K$, a therapeutic agent for respiratory distress syndrome, in aqueous monolayers with phospholipids. Biochem 2003;42:9446–52. [PubMed: 12899632]
24. Martinez-Gil L, Perez-Gil J, Mingarro I. The surfactant peptide KL_4 sequence is inserted with a transmembrane orientation into the endoplasmic reticulum membrane. Biophys J 2008;95:L36–L38. [PubMed: 18621816]
25. Terzi E, Holzemann G, Seelig J. Interaction of Alzheimer beta-amyloid peptide(1–40) with lipid membranes. Biochem 1997;36:14845–52. [PubMed: 9398206]
26. Ramamoorthy A, Thennarasu S, Lee DK, Tan A, Maloy L. Solid-state NMR investigation of the membrane-disrupting mechanism of antimicrobial peptides MSI-78 and MSI-594 derived from magainin 2 and melittin. Biophys J 2006;91:206–16. [PubMed: 16603496]
27. Wieprecht T, Apostolov O, Beyermann M, Seelig J. Thermodynamics of the alpha-helix-coil transition of amphipathic peptides in a membrane environment: implications for the peptide-membrane binding equilibrium. J Mol Biol 1999;294:785–94. [PubMed: 10610796]
28. Veldhuizen R, Nag K, Orgeig S, Possmayer F. The role of lipids in pulmonary surfactant. BBA-Mol Basis Dis 1998;1408:90–108.
29. Antharam VC, Elliott DW, Mills FD, Farver RS, Sternin E, Long JR. The penetration depth of surfactant peptide KL_4 into membranes is determined by fatty acid saturation. Biophys J 2009;96:4085–98. [PubMed: 19450480]
30. Ying WW, Irvine SE, Beekman RA, Siminovitch DJ, Smith SO. Deuterium NMR reveals helix packing interactions in phospholamban. J Am Chem Soc 2000;122:11125–11128.
31. Gottler LM, Bea RD, Shelburne CE, Ramamoorthy A, Marsh ENG. Using fluorous amino acids to probe the effects of changing hydrophobicity on the physical and biological properties of the beta-hairpin antimicrobial peptide protegrin-1. Biochem 2008;47:9243–9250. [PubMed: 18693751]
32. Gottler LM, Lee HY, Shelburne CE, Ramamoorthy A, Marsh ENG. Using fluorous amino acids to modulate the biological activity of an antimicrobial peptide. Chembiochem 2008;9:370–373. [PubMed: 18224631]
33. Samuel-Landtiser M, Zachariah C, Williams CR, Edison AS, Long JR. Incorporation of isotopically enriched amino acids. Curr Protoc Protein Sci Chapter 2007;26 Unit 26 3.
34. Chen PS, Toribara TY, Warner H. Microdetermination of phosphorus. Anal Chem 1956;28:1756–1758.
35. Tiburu EK, Karp ES, Dave PC, Damodaran K, Lorigan GA. Investigating the dynamic properties of the transmembrane segment of phospholamban incorporated into phospholipid bilayers utilizing H-2 and N-15 solid-state NMR spectroscopy. Biochem 2004;43:13899–13909. [PubMed: 15518538]
36. Abu-Baker S, Lu JX, Chu SD, Brinn CC, Makaroff CA, Lorigan GA. Side chain and backbone dynamics of phospholamban in phospholipid bilayers utilizing H-2 and N-15 solid-state NMR spectroscopy. Biochem 2007;46:11695–11706. [PubMed: 17910421]
37. DeLano, WL. DeLano Scientific, LLC. Palo Alto, CA, USA: 2008.
38. Vogt B, Ducarme P, Schinzel S, Brasseur R, Bechinger B. The topology of lysine-containing amphipathic peptides in bilayers by circular dichroism, solid-state NMR, and molecular modeling. Biophys J 2000;79:2644–2656. [PubMed: 11053137]
39. Perkins WR, Dause RB, Parente RA, Minchey SR, Neuman KC, Gruner SM, Taraschi TF, Janoff AS. Role of lipid polymorphism in pulmonary surfactant. Science 1996;273:330–2. [PubMed: 8662513]

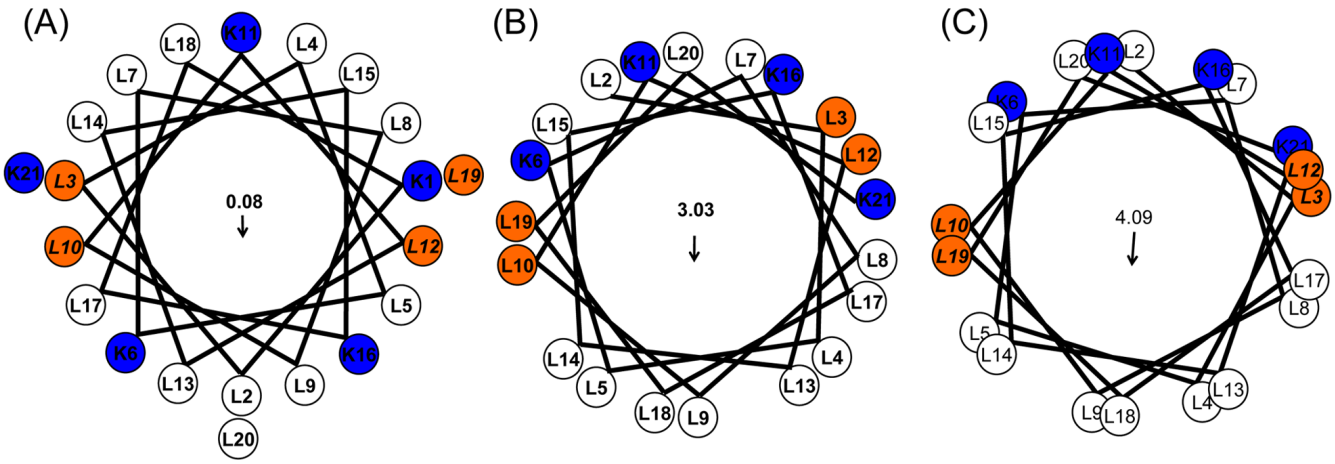

Figure 1.

Helical wheel plots of KL_4 with varying (ϕ, ψ torsion angles. (A) Wheeleratedgen assuming a canonical α-helix (ϕ, ψ = −63°, −42°); (B) using the average torsion angles determined in POPC:POPG vesicles (ϕ, ψ = −105°, −30°); and (C) using the average torsion angles observed in DPPC/POPG vesicles (ϕ, ψ = −63°, −81°). Arrows indicate the net hydrophobic moments resulting from the distribution of charged lysine sidechains on the helix surface. The first lysine is not shown in (B) and (C) as NMR data indicate the N-terminus is less structured relative to the rest of the helix.

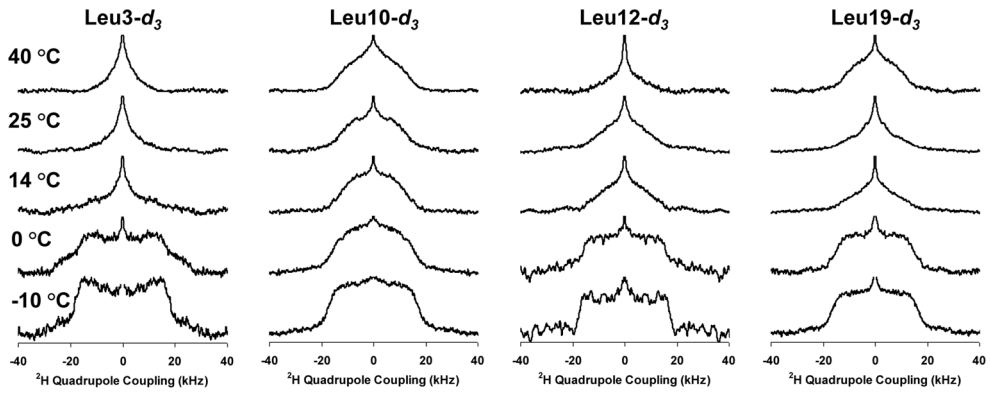

Figure 2.

Deuterium NMR spectra as a function of temperature for the various 5-d_3-L-Leucine enriched position in KL_4 in samples containing POPC/POPG vesicles.

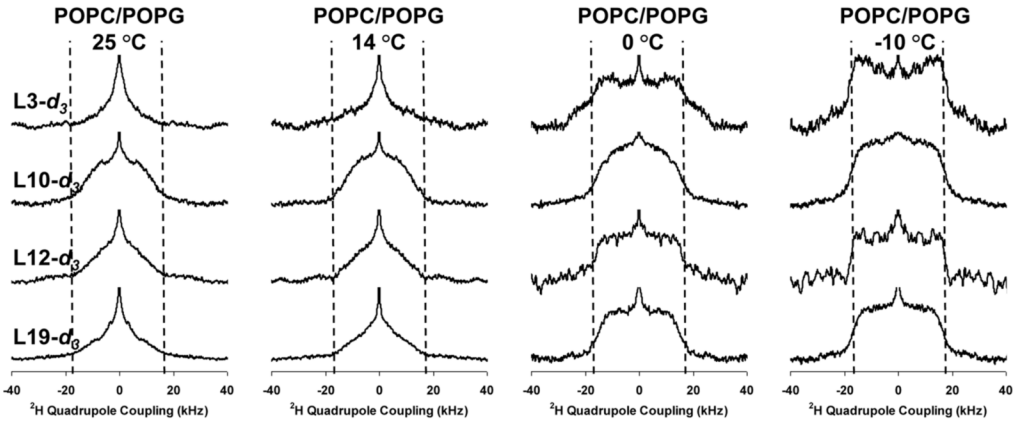

Figure 3.
Deuterium NMR spectra as a function of label position for the various 5-d_3-L-Leucine enriched position in KL_4 in samples containing POPC/POPG vesicles.

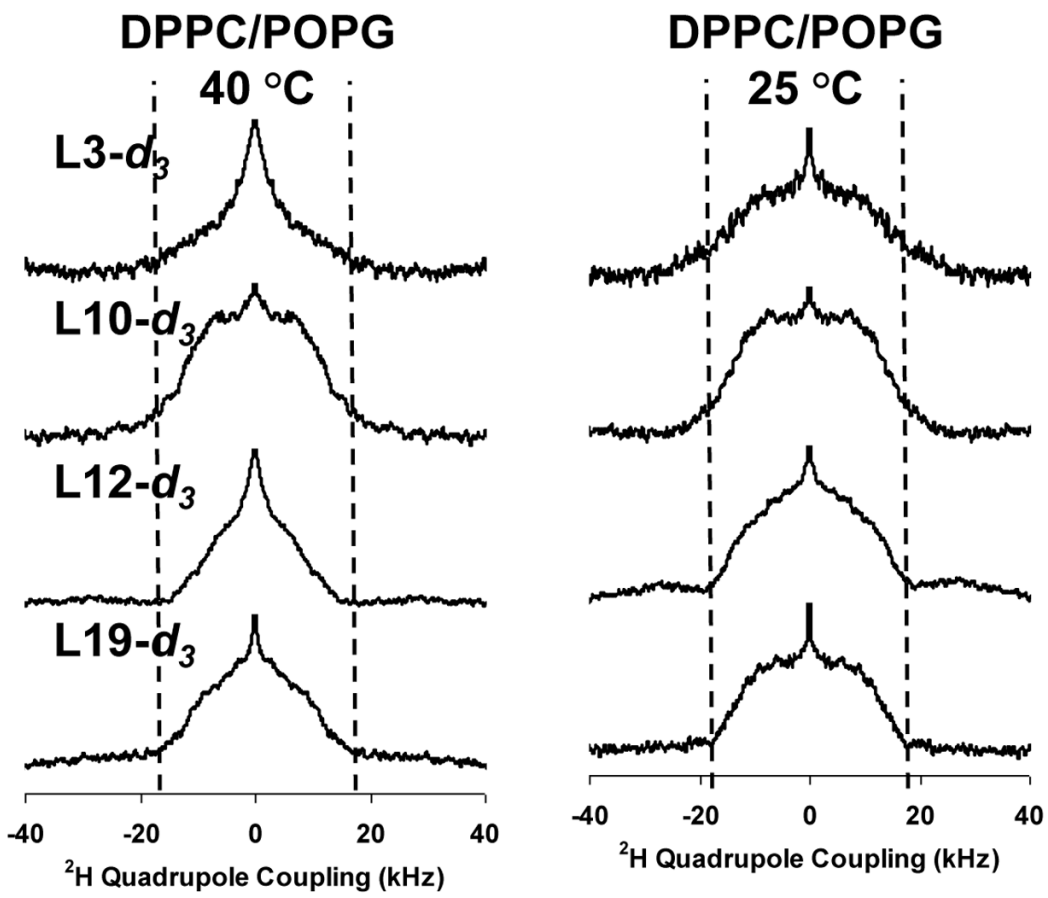

Figure 4.
Deuterium NMR spectra as a function of label position for the various 5-d_3-L-Leucine enriched position in KL_4 in samples containing DPPC/POPG vesicles.

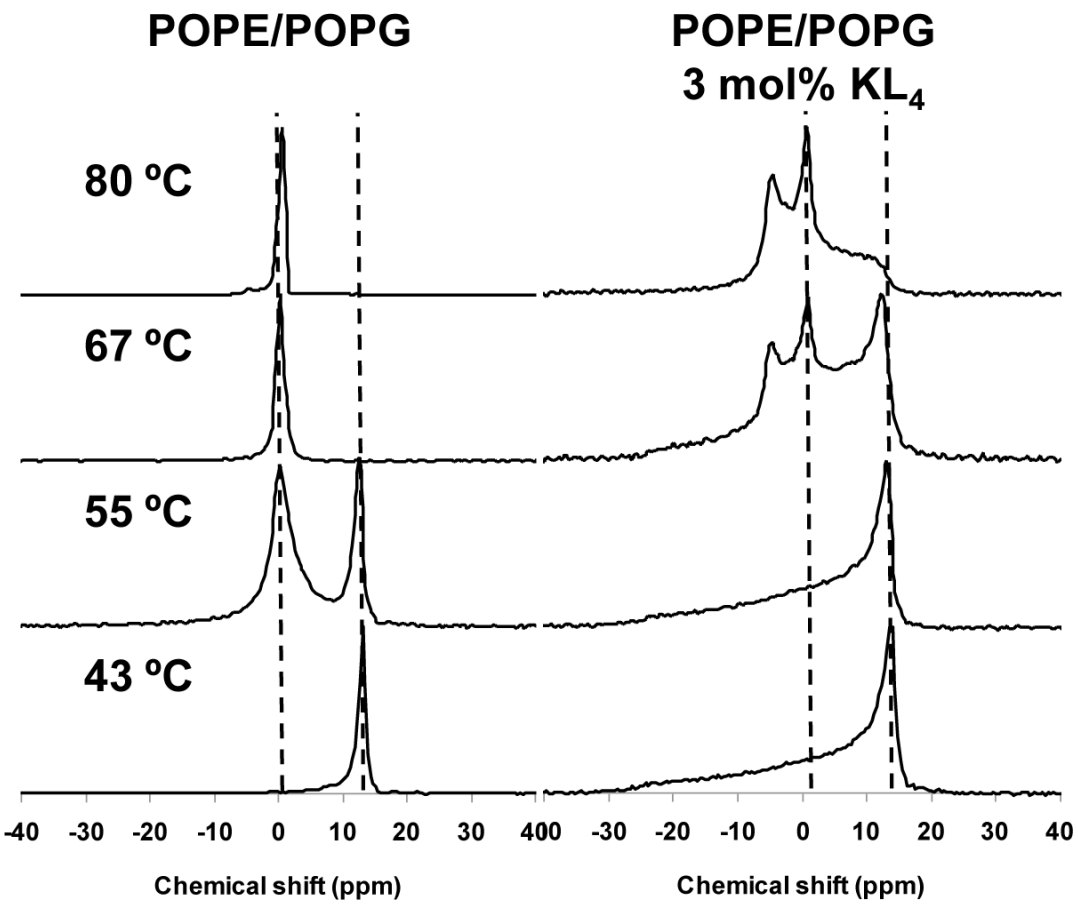

Figure 5.
Phosphorous NMR spectra as a function of temperature for 3:1 POPE/POPG lipid vesicles with and without 3 mol% KL_4.

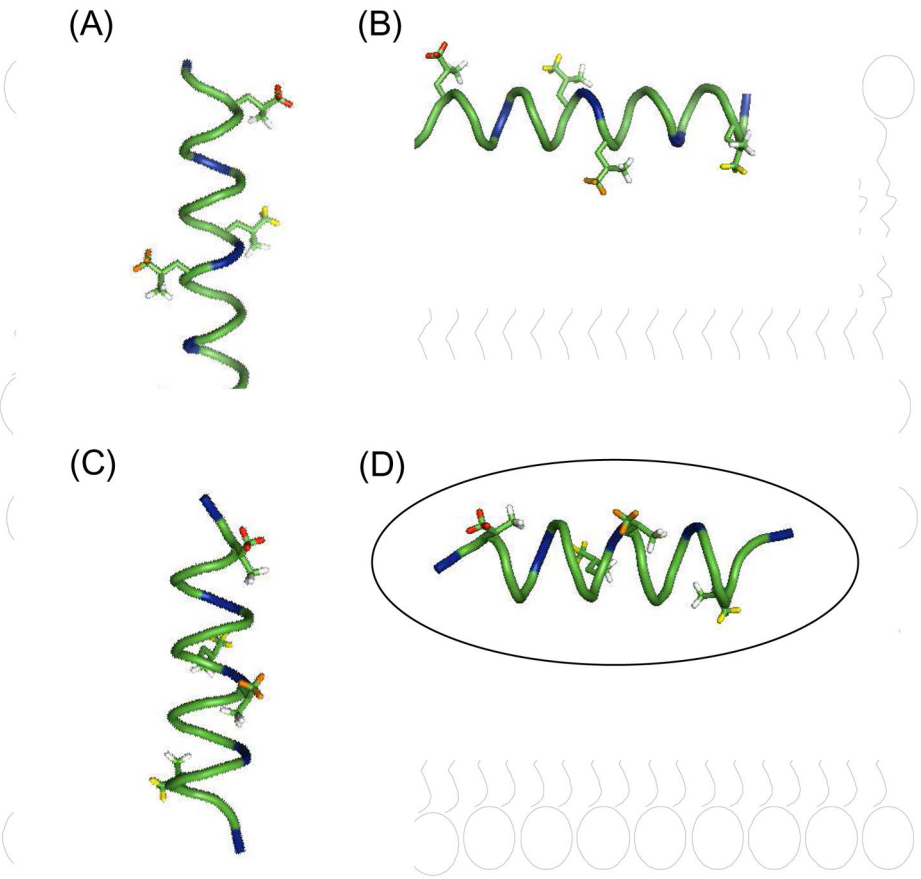

Figure 6.

Model of the possible structures and orientations of KL_4 in the lipid bilayer: (A) a canonical α-helix in a transmembrane orientation; (B) an α-helix in the plane of the bilayer; (C) the helix from Figure 1c in a transmembrane orientation; and (D) the helix from Figure 1C lying in the plane of the bilayer. The deuterated leucine methyl groups used in this study are color-coded with respect to their relative dynamics in POPC./POPG at 40 °C with Leu3 (red) > Leu 12 (orange) > Leu10 ≈ Leu19 (yellow).